JOURNAL OF AGRICULTURAL AND FOOD CHEMISTRY

Article

Cite This: J. Agric. Food Chem. 2019, 67, 4071−4079

pubs.acs.org/JAFC

Fabricating an Acetylcholinesterase Modulated UCNPs-Cu^{2+} Fluorescence Biosensor for Ultrasensitive Detection of Organophosphorus Pesticides-Diazinon in Food

Pingyue Wang,[†] Huanhuan Li,[†] Md Mehedi Hassan,[†] Zhiming Guo,[†] Zheng-Zhu Zhang,[‡] and Quansheng Chen*[,†]

[†]School of Food and Biological Engineering, Jiangsu University, Zhenjiang 212013, China

[‡]State Key Laboratory of Tea Plant Biology and Utilization, Anhui Agricultural University, Hefei 230036, China

Supporting Information

ABSTRACT: In this study, a highly sensitive upconversion fluorescence (FL) biosensor was developed for the detection of organophosphorus pesticides (OPs) based on an acetylcholinesterase (AChE) modulated FL "off−on−off" strategy. The luminescence of synthesized UCNPs could be quenched strongly by Cu^{2+} due to an energy transfer effect. Upon addition of AChE and acetylthiocholine (ATCh), the enzymatic hydrolysate (thiocholine) could seize Cu^{2+} from UCNPs-Cu^{2+} mixture, resulting in the quenched FL triggered on. OPs could irreversibly impede the activity of AChE, which caused the formation of thiocholine to decrease, thus, reduced the recovery of FL. Under the optimum conditions, a linear detection range from 0.1 to 50 ng/mL was achieved for the representative OPs (diazinon) with LOD of 0.05 ng/mL. Furthermore, the ability of the biosensor to detect OPs was also confirmed in adulterated environmental and agricultural samples. In validation analysis, the proposed sensor showed satisfactory results ($p > 0.05$) with GC−MS.

KEYWORDS: *upconversion nanoparticles, fluorescence, Cu^{2+}, acetylcholinesterase, organophosphorus pesticides*

1. INTRODUCTION

In modern agriculture, pesticides are extensively exploited to protect crops against pests and insects.[1] Comparatively owing to the high effectiveness toward insect and easily degradable under the environmental condition, OPs such as phorate, diazinon, malathion, etc. have been grouped as most commonly applied pesticides throughout the world to ensure the high production of crops.[2−5] However, the over use of pesticides has also raised serious public health concern because the inappropriate disposal of OPs causes a potential threat to human health even at very low concentration through the contamination of water, atmosphere, and agricultural products.[6,7] It is estimated that every year approximately two million people died of OPs poisoning.[8] The high toxicity of OPs is owing to their ability to irreversibly inhibit the catalytic activity of acetylcholinesterase (AChE), a critical central-nervous enzyme, causing the accumulation of the neurotransmitter acetylcholine *in vivo*. The overaccumulation of acetylcholine can lead to damage to human health or even fatal consequences.[9−11] Therefore, it is of great significance to develop a rapid, reliable, and sensitive method for monitoring and quantification of OPs residues in food to ensure safety and protect human health.

Various techniques have been designed and employed for the quantification of OPs over the past decades including high performance liquid chromatography (HPLC),[12] thin-layer chromatography,[13] enzyme-linked immunosorbent assays (ELISAs),[14] gas chromatography−mass spectrometry (GC−MS),[15] electrochemical assay,[16] colorimetric assay,[17] surface-enhanced Raman scattering,[18] and chemiluminescence assay.[19] Albeit, the aforementioned techniques showed good selectivity and sensitivity to the analytes, several shortcomings of them still exist, such as chromatographic techniques often require relatively expensive instruments and tedious sample pretreatment processes, the immunoassays typically rely on the involvement of specific antibodies.[20,21] On the contrary, the fluorescence-based analytical technique has attracted extensive investigative attention in recent years, owing to its short detection time, high sensitivity and selectivity, and low detection limit.[22,23] For example, Liu and co-workers fabricated a rhodamine B-covered gold nanoparticle (RB-AuNP) for detecting organophosphorus in complex solutions.[24] Nanda Kumar et al. designed an unmodified silver nanoparticles for the detection of malathion.[25] Minsu Kim's group employed quantum dots (QDs) as fluorescence reporters for paraoxon detection.[26] In addition, several studies also reported for the detection of organophosphorous pesticides using carbon dots as fluorescence reporters.[27−30] However, most of these fluorescence nanosensors for OPs detection are based on organic fluorescence dye, quantum dots, and carbon dots, but there still exist some limitations among these techniques for application in real food. Organic fluorophores and dyes because of their variable chemical structure and down-conversion fluorescence characteristics are usually associated with poor water-solubility, photobleaching, and photodamage issues.[31] Similarly, the use of highly toxic inorganic reagents in the synthesis of quantum dots (QDs) and the interference of

Received: December 24, 2018
Revised: February 21, 2019
Accepted: March 19, 2019
Published: March 19, 2019

Downloaded via UNIV OF GLASGOW on July 18, 2020 at 11:55:42 (UTC).
See https://pubs.acs.org/sharingguidelines for options on how to legitimately share published articles.

ACS Publications © 2019 American Chemical Society

DOI: 10.1021/acs.jafc.8b07201
J. Agric. Food Chem. 2019, 67, 4071−4079

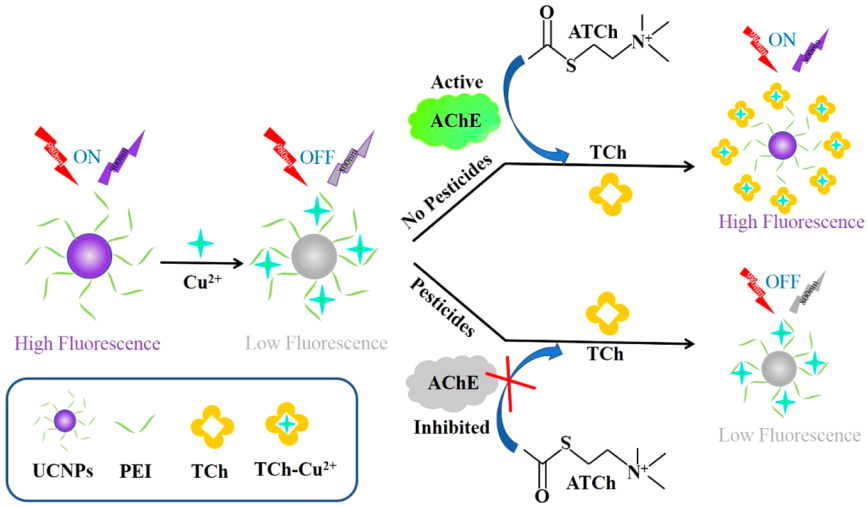

Figure 1. Schematic description of the acetylcholinesterase modulated UCNPs-Cu^{2+} fluorescence biosensor for organophosphorus pesticides.

background autofluorescence caused by its shorter wavelength excitation properties also limit its application in complex food systems.[32] Conversely, the carbon dots achieved more attention in the sense of required chemicals used for synthesis; however, they suffered in rapid on-site detection on account of their prolonged synthesis time. Thus, developing a novel fast fluorescence sensor capable of overcoming the interference of autofluorescence and photobleaching for efficient detection of OPs in real samples is vitally important.

Lanthanide-doped upconversion nanoparticles (UCNPs) have the unique photophysical properties that can emit strong light of shorter wavelength with the excitation of near-infrared (NIR) photons, which lead to many studies in diagnostics and biomedical imaging as biolabels.[33] Compared with traditional down-conversion organic luminescence materials, UCNPs possess several unique advantages such as the large antiStokes shifts, high quantum yields, long lifetimes, no photobleaching and nonblinking emission, high chemical stability, and low cytotoxicity.[34] Most importantly, the special upconverting luminescence properties of UCNPs allow them to avoid the interference of background autofluorescence as well as improve the detection sensitivity. All of these attractive advantages of UCNPs make them become more ideal fluorescence materials compared to other conventional fluorophores. In the past few years, the successful application of UCNPs in different pesticides detection has been reported.[35−37] However, most of them required complicated chemical processes to construct the biosensor such as amino or carboxyl modification of UCNPs surface, synthesis of specific fluorescent quenchers, or immobilization of recognition molecules. To the best of our knowledge, still no study has been reported for the determination of OPs in food samples based on the quenching effect of copper ions on UCNPs.

Herein, we have developed a sensitive fluorescence biosensor to detect trace level of OPs in food based on the fluorescence (FL) quenching of UCNPs by copper ions (Cu^{2+}) and the specific recognition ability of AChE enzyme to OPs. The detailed detection strategy of the proposed platform for OPs has been schematically depicted in Figure 1. $NaGdF_4$: Yb/Tm UCNPs prepared by one-step solvothermal route were capped with branched polyethylenimine (PEI) on their surfaces. It was observed that the upconversion luminescence of UCNPs was quenched strongly by Cu^{2+} because of the coordination of Cu^{2+} to the amino groups of PEI. Upon addition of AChE and acetylthiocholine (ATCh) into the aforementioned UCNPs-Cu^{2+} mixed system, ATCh catalytically hydrolyzed by AChE to produce thiocholine (TCh) and acetic acid, the produced TCh could preferentially bond with copper ions from UCNPs-Cu^{2+} mixture resulting in the quenched fluorescence of UCNPs was retrieved. However, OPs act as an enzyme inhibitor and can strongly suppress the activity of AChE, causing the generation of TCh to be decreased and the fluorescence signal to be quenched again. On the basis of the fluorescence "off−on−off" strategy, an AChE modulated upconversion luminescence biosensor for the highly sensitive detection of OPs has been designed. The proposed method not only showed great potential for monitoring of organophosphorus pesticide levels in real samples, but also provided a novel strategy for other enzyme inhibitor screening.

2. MATERIALS AND METHODS

2.1. Chemicals. Branched polyethylenimine (PEI, MW ∼25 000) and acetylcholinesterase (AChE) were bought from Sigma-Aldrich (U.S.A.). Rare-earth nitrate used in this work, including Ytterbium(III) nitrate pentahydrate (Yb $(NO_3)_3{\cdot}5H_2O$), Thulium(III) nitrate hexahydrate ($Tm(NO_3)_3{\cdot}6H_2O$), and Gadolinium(III) nitrate hexahydrate ($Gd(NO_3)_3{\cdot}6H_2O$) were of 99.99% purity and obtained from Aladdin Industrial Co. Ltd. (Shanghai, China). Sodium chloride (NaCl, ≥ 99.5%), ethylene glycol (EG, 99%), ammonium fluoride (NH_4F), copper(II) chloride dihydrate ($CuCl_2{\cdot}2H_2O$, 99.99%), acetylthiocholine iodide (ATChI, BR), ethanol, and phosphate buffered saline (PBS, pH 7.4) were obtained from Sinopharm Chemical Reagent Co., Ltd. (Shanghai, China). All pesticides were purchased from Pesticides Research Institute Co. Ltd. (Shanghai, China). All starting chemicals for this experiment were analytical grade and used without any purification. Deionized water with good resistivity (18.2 MΩ cm) was used throughout the experiment and obtained from the Smart-S ultrapure water system.

2.2. Instruments and Characterizations. A JEOL JEM-2100 (HR) high-resolution transmission electron microscope (HR-TEM; JEOL Ltd., Japan) at 200 kV accelerating voltage was used to determine the size and morphology of UCNPs. Sample dispersions were dropped on the surface of a copper grid to perform TEM characterization. X-ray powder diffraction (XRD) patterns were used to characterize the crystalline phases of UCNPs and measured on a D8 Advance (Germany) X-ray diffractometer at a 5°/min scanning rate in the 2θ range from 10° to 60°. Agilent 8453 Ultraviolet−visible (UV−vis) spectrophotometer (Agilent Technologies Inc.) was used

DOI: 10.1021/acs.jafc.8b07201
J. Agric. Food Chem. 2019, 67, 4071−4079

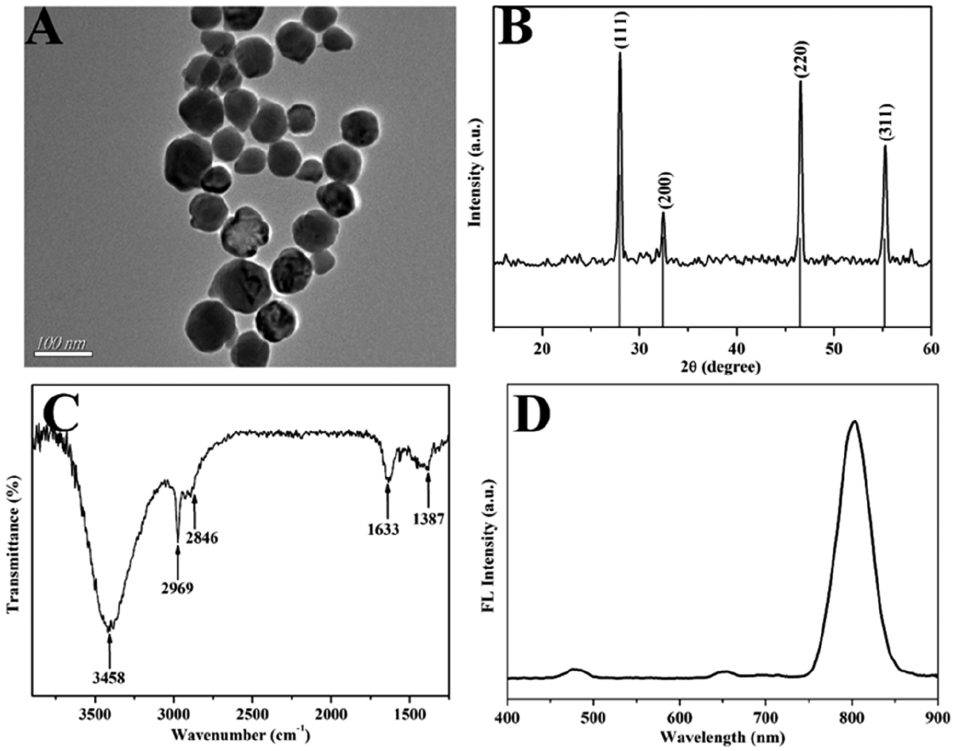

Figure 2. (A) TEM image of UCNPs. (B) XRD pattern of UCNPs. (C) FT-IR spectroscopy of UCNPs. (D) Fluorescent emission spectra of UCNPs under 980 nm excitation.

to record the UV−vis absorption spectrum. Upconversion fluorescence emission spectra were collected using a combined fluorescence spectrum measurement system including PMTH-S1-CR131A side-on photomultiplier tube, SAC sample house, HVC1800 high-voltage power supply, Omni-λ300 grating monochromator, DCS103 data acquisition equipment, and an external adjustable 980 nm continuous-wave laser (CLOT Co., Ltd. China). A Nicolet Nexus 470 Fourier transform infrared spectroscopy (Thermo Electron Co., U.S.A.) was used to collect the Fourier transform infrared (FT-IR) spectra of the prepared bionanoparticles. The GC−MS method was developed on a Thermo ITQ1100 gas chromatography−mass spectrometer (Thermo Fisher Scientific Co., U.S.A.).

2.3. Preparation of Standard Stock Solution. The solution of ATCh with the concentration of 100 mM was freshly prepared by dissolving 0.145 g of standard ATCh in 5 mL of deionized water and shaken well. To avoid the possible hydrolysis of it, the stock solution should not be used more than 2 weeks after preparation. The AChE solution (100 unit/mL) was prepared by dissolving a suitable amount of standard in phosphate buffered saline (PBS, pH 7.4) and used within 4 days after preparation to ensure the activity of the enzyme. Then 100 μg/mL of different pesticides stock solution was prepared from the standard chemical with cyclohexane for fluorescence and GC−MS analysis. All of these working standard stock solutions were stored in a refrigerator at 4 °C for further use.

2.4. Synthesis of PEI-Capped Upconversion Nanoparticles. PEI-capped water-soluble $NaGdF_4$: Yb/Tm UCNPs were prepared using a modified literature procedure via the solvothermal processes.[38] In brief, 2.4 mmol of NaCl and PEI (0.4 g) were mixed in 18.0 mL of EG under stirring. Then $Gd(NO_3)_3{\cdot}6H_2O$ (325 mg, 0.72 mmol), $Yb(NO_3)_3{\cdot}5H_2O$ (213 mg, 0.474 mmol), $Tm(NO_3)_3{\cdot}6H_2O$ (2.7 mg, 0.006 mmol) were introduced to the above mixture and continued to agitate approximately 30 min. When the solution was observed to become transparent, NH_4F (231 mg, 6.24 mmol) in 12 mL of EG was added to the above mixture and kept stirring for another 10 min at room temperature. Subsequently, the mixture was relocated into a 50 mL Teflon-lined stainless steel vessel and treated at 200 °C for 1.5 h. Then the system was cooled down to ambient temperature naturally. The yielded PEI-capped UCNPs were collected by centrifugation at 10 000 rpm for 5 min, then washed three times with DI water and ethanol. Finally, the PEI-capped UCNPs were obtained by drying at 60 °C for 12 h under vacuum and stored for further experimental operation.

2.5. OPs Determination. The commonly used diazinon was selected as the representative model for OPs. The specific detection process was as follows. Different concentrations of pesticides (50 μL) prepared from the stock solution were mixed with AChE solution (25 mU/mL, 50 μL), which were incubated at 37 °C for 25 min under dark condition. Afterward, 10 mM ATCh (50 μL) was mixed into the above mixture and incubated for another 30 min at 37 °C. Next, 1 mL of prepared UCNPs (0.18 mg/mL), 100 μL of Cu^{2+} (5 μM), and 750 μL of Milli-Q water were added to the above reaction mixture. Subsequently, the final mixture was incubated again for 6 min at room temperature for the collection of fluorescence emission intensity at 800 nm using the assembled fluorescence spectrometer with excitation wavelength at 980 nm. Blank experiment was conducted using cyclohexane.

2.6. Analysis of Spiked Samples. Tap water, lake water, apple, pear, and green tea powder were selected as the sample matrix to monitor the diazinon residue levels for evaluating the feasibility of this developed sensor in the real sample analysis. The apples, pears, and green tea powder were purchased from a local supermarket (Zhenjiang, China), tap water was taken from laboratory water outlet directly, and lake water was collected from Yudai Lake, Zhenjiang, China. The pretreatment methods of them were as follows. Tap water and lake water (10 mL) were centrifuged and filtered through a 0.22 μm nylon membrane to discard any unwanted foreign materials. The apple samples and pear samples were finely chopped first; then the edible parts were taken and blended at high speed for 5 min. Twenty grams of the above crushed sample was mixed with 40 mL of acetonitrile and homogenized for 5 min, and the mixture was centrifuged at 3000 rpm for 5 min. The obtained supernatant was filtered through a 0.22 μm membrane to remove any insoluble residues. Green tea powder (10 g) was mixed with 30 mL of acetonitrile solution in a 50 mL centrifuge tube and homogenized for 5 min. Then the content was centrifuged at 4200 rpm for 5 min and filtered through a 0.22 μm membrane. The extraction procedure was

DOI: 10.1021/acs.jafc.8b07201
J. Agric. Food Chem. 2019, 67, 4071−4079

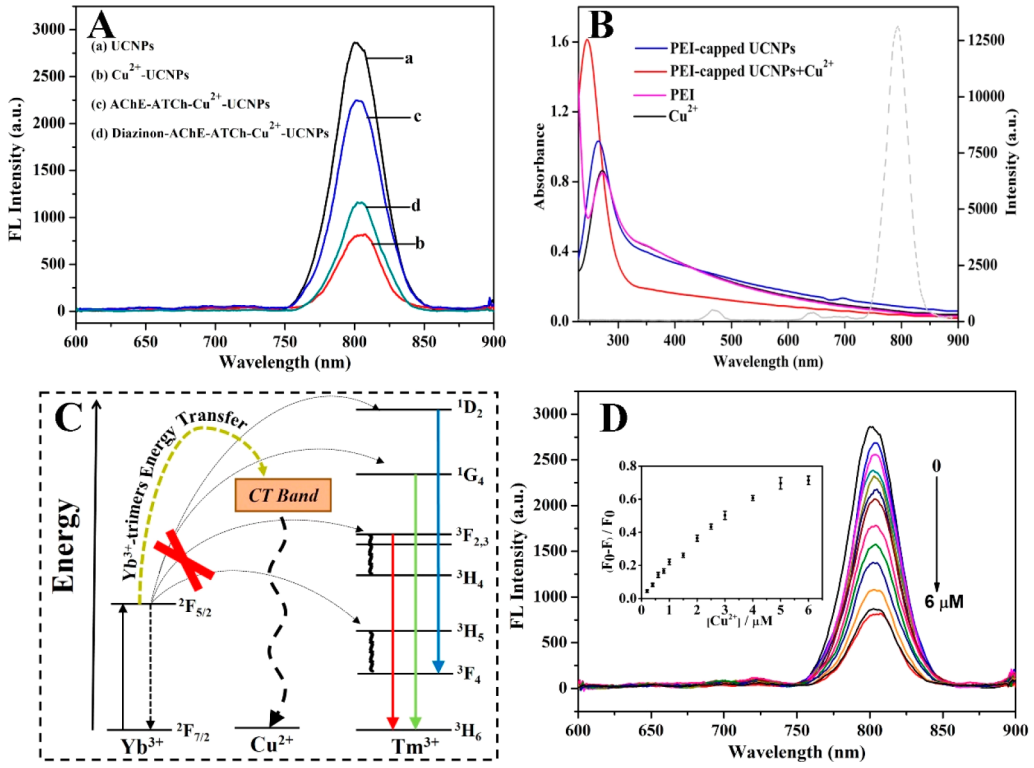

Figure 3. (A) Fluorescence emission spectra of (a) UCNPs solution, (b) Cu^{2+}-UCNPs solution, (c) AChE-ATCh-Cu^{2+}-UCNPs solution, (d) Diazinon-AChE-ATCh-Cu^{2+}-UCNPs solution. (B) UV−vis absorption spectra of PEI-capped UCNPs (blue line), PEI-capped UCNPs+Cu^{2+} (red line), PEI (pink line), Cu^{2+} (black line), and FL spectrum of PEI-capped UCNPs (dot line). (C) Plausible energy transfer mechanism from UCNPs to Cu^{2+}. (D) Fluorescence spectra of UCNPs with different concentration of Cu^{2+} (0, 0.2, 0.4, 0.6, 0.8, 1, 1.5, 2, 2.5, 3, 4, 5, and 6 μM). Inset shows the plot of fluorescence quenching efficiency versus Cu^{2+} concentration.

repeated three times and the extracts were combined. Finally, different volumes of diazinon stock solutions were spiked into the above-pretreated tap water, lake water, apple extract, pear extract, and green tea extract, respectively, to obtain the final concentrations of diazinon in the range of 0 to 20 ng/mL (or ng/g) and dried by using rotary evaporator under nitrogen gas flow to evaporate the acetonitrile. Then the dried residue was dissolved in cyclohexane and quantitatively detected by the section 2.5 developed procedure. Each spiked concentration was repeated three times.

2.7. Analysis of Authentic Samples. The apples sprayed with different amount of diazinon were collected from a farm in Zhenjiang, and they were considered as the authentic sample to evaluate the UCNPs-Cu^{2+} probe for the detection of OPs pesticide residues in actual food. The concentrations of diazinon in the samples were detected by this enzyme probe and GC−MS method simultaneously. After processing of apples according to the Chinese national standard fruits pretreatment method, the detection procedures of the prepared nanosensor were carried out as the steps of the spiked samples and GC−MS was performed according to the procedure suggested in the Chinese national food safety standards guideline on determination of pesticides and related chemicals residues in fruits and vegetables (GB 23200.8−2016).

3. RESULTS AND DISCUSSION

3.1. Characterization of PEI-Capped UCNPs. To access the size, morphology, and optical feature of the synthesized PEI-capped UCNPs, a series of characterization such as, TEM, XRD, FT-IR, and fluorescence spectra were conducted. As shown in Figure 2, the TEM image (Figure 2A) revealed that the as-prepared PEI-capped UCNPs have good dispersity in water solution and are fairly spherical in size. As shown in Figure 2B, the XRD pattern of PEI-capped UCNPs showed that all the diffraction peaks were corresponded to the α-$NaGdF_4$ crystals (JCPDS no. 27−0697), indicating that the synthesized nanomaterials were highly crystalline in nature. In addition, the surface properties of PEI-capped UCNPs were further analyzed by FT-IR spectroscopy as captured in Figure 2C. The high-intensity peaks at 3458 and 1633 cm^{-1} were ascribed to the stretching and bending vibration of N−H, respectively. Meanwhile, the transmission bands centered at 2969 and 2846 cm^{-1} were assigned to the asymmetric and symmetric stretching vibrations of the methylene group ($-CH_2-$) in the long alkyl chain, respectively. In addition, the peak at 1387 cm^{-1} corresponded to the stretching vibrations of C−N bonds. All of these characteristic peaks suggested that the PEI molecules were successfully capped on the surface of UCNPs, which resulted in high water solubility of the synthesized UCNPs. Figure 2D showed the upconversion fluorescence spectra of PEI-capped UCNPs under 980 nm laser excitation. Three characteristic emission peaks at 480, 652, and 800 nm were observed, which could be assigned to the $^1D_2 \rightarrow {}^3F_4$, $^1G_4 \rightarrow {}^3H_6$, $^3F_{2,3} \rightarrow {}^3H_6$ transitions of Tm^{3+} ions, respectively.[39] It was seen that the fluorescence peak at 800 nm was much higher than all the other luminescence bands as well, thereby which was employed as the report signal throughout the experiment. Furthermore, we also investigated the chemical and photostability of the prepared PEI-capped UCNPs under different environmental conditions. As shown in Figure S1A, the FL intensity of the synthesized PEI-capped UCNPs remained almost unchanged within 2 h. It could be obviously found that the FL emission intensity of PEI-capped UCNPs at 800 nm showed negligible decline over different temperature (Figure S1B), pH (Figure S1C), and concentration of salt (Figure S1D). These results

DOI: 10.1021/acs.jafc.8b07201
J. Agric. Food Chem. 2019, 67, 4071−4079

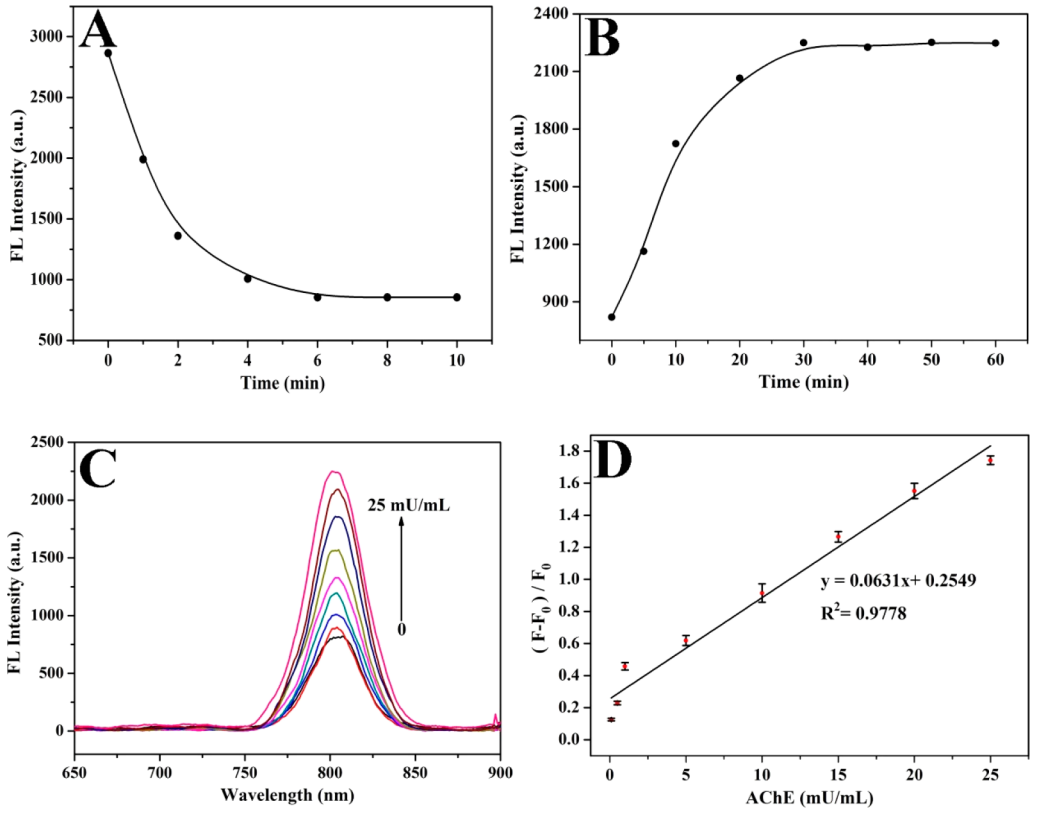

Figure 4. (A) Optimization the incubation time for the interaction between UCNPs and Cu^{2+}. (B) Optimization of the incubation time for the interaction between ATCh and AChE. (C) Fluorescence spectra of UCNPs-Cu^{2+}-ATCh system in the presence of different concentrations (0 to 25 mU/mL) of AChE. (D) Plot of fluorescence enhancement efficiency versus AChE concentration.

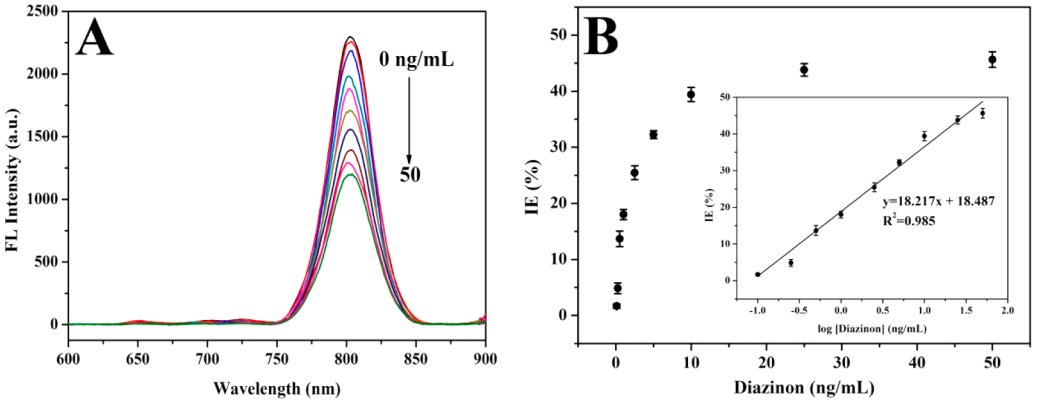

Figure 5. (A) Fluorescence spectra of the UCNPs-Cu^{2+}-AChE-ATCh system in the presence of different concentrations of diazinon. (B) Plot of inhibition efficiency with the different concentrations of diazinon (0.1, 0.25, 0.5, 1, 2.5, 5, 10, 25, and 50 ng/mL). Inset: the linear relationship with the logarithmic concentration of diazinon.

indicated that the obtained UCNPs possessed excellent stability, letting them promise as a suitable candidates to construct efficient ratiometric fluorescence sensor.

3.2. Detection Scheme of OPs Sensor. The basic principle of the designed UCNPs-based OPs biosensor consists of the following three parts: (1) quenching of the fluorescence of PEI-capped UCNPs by copper ion; (2) AChE can hydrolyze its active substrate ATCh to produce thiocholine, which possesses stronger affinity to Cu^{2+} resulting in quenching impaired; (3) organophosphorus pesticides can effectively inhibit the activity of AChE enzyme consequently quenching retrieved. As shown in Figure 3A, PEI-capped UCNPs solution performed a highest FL signal at 800 nm under the laser excitation of 980 nm (curve a); the FL emission intensity of PEI-capped UCNPs could be remarkably quenched via the energy transfer (ET) effect when mixed with Cu^{2+} (curve b); importantly, upon introduction of both ATCh and AChE into the ensemble solution, an obvious recovered FL enhancement appeared (curve c). This was caused by the fact that thiol group of thiocholine yielded from ATCh under the catalytic hydrolysis of AChE showed higher binding affinity to Cu^{2+},[40] resulting in thiocholine captured the Cu^{2+} from the PEI-capped UCNPs-Cu^{2+} nanoassembly, accompanied by the recovery of quenched FL of PEI-capped UCNPs. However, when diazinon was added into the detecting system, the FL quenching of UCNPs happened again (curve d). This principle

DOI: 10.1021/acs.jafc.8b07201
J. Agric. Food Chem. 2019, 67, 4071−4079

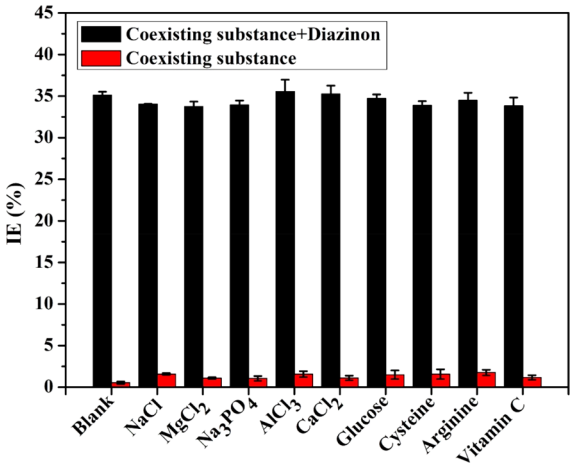

Figure 6. Inhibition efficiency of the UCNPs-Cu^{2+}-AChE-ATCh-diazinon system with the interfering substances. The concentrations of diazinon and other substances are 10 ng/mL and 10 μg/mL.

can be elucidated as follows: diazinon as one kind of typical OPs, which is capable of suppressing the activity of AChE, then the efficiency of AChE to catalyze the hydrolysis of ATCh was enfeebled and the generation of thiocholine was obviously reduced, leading to the FL of PEI-capped UCNPs quenched by Cu^{2+} again. To determine the feasibility of this biosensor for OPs sensing, the influences of several related factors were also investigated. From Figure S2A, it is obvious that the changes of FL intensity were not noticeable when ATCh, AChE, or diazinon was separately incubated with PEI-capped UCNPs under the identical experimental condition, and the FL intensity of UCNPs+AChE, UCNPs+ATCh, UCNPs+diazinon system was similar to that of the UCNPs. In addition, the FL emission spectrum of UCNPs-Cu^{2+} ensemble solution was recorded when the UCNPs-Cu^{2+} mixture was individually incubated with AChE, ATCh and/or diazinon under the identical experimental condition (Figure S2A). The results indicated that their fluorescence intensity was almost unchanged from the UCNPs-Cu^{2+} mixed solution. Consequently, all of these results suggested that the factors mentioned above were unable to influence the experimental results and the proposed strategy for OPs sensing is feasible.

To study the basic principle of Cu^{2+}-induced photoluminescence quenching, we first investigated the FL emission spectrum and the UV−vis absorption spectrum of PEI-capped UCNPs and Cu^{2+} related materials, respectively. Figure 3B showed the UV−vis absorption peak of Cu^{2+} before and after addition of PEI-capped UCNPs, a shift of the peak position from 280 to 250 nm was observed after addition of PEI-capped UCNPs, indicative of the formation of cupric amine coordinates base on the interaction between PEI-capped UCNPs and Cu^{2+}. However, it was also observed that the upconversion FL emission peak at 800 nm of PEI-capped UCNPs were not overlapped with the ultraviolet absorption band of Cu^{2+}. On the basis of the consideration of these above two reasons, it was conspicuous that inner-filter effect (IFE) was not the dominating mechanism for the quenching of the FL. In addition, the Cu^{2+}-induced quenching of luminescence in upconversion nanoparticle was possibly due to the ET effect as reported.[41,42] Figure 3C showed the energy level diagram and a schematic representation of the cooperative energy transfer from Yb^{3+} to Cu^{2+}, in which the energy levels of copper ions were obtained from the literature.[43] Upon 980 nm

Table 1. Determination of Diazinon in Various Spiked Water and Food Samples[a]

		intraday (n = 3)						
		day 1		day 2		day 3		
sample	spiked levels (ng/mL or ng/g)	found ± SD (ng/mL or ng/g)	recovery (%)	found ± SD (ng/mL or ng/g)	recovery (%)	found ± SD (ng/mL or ng/g)	recovery (%)	interday RSD (%) (n = 9)
tap water	0							
	0.5	0.5 ± <0.1	94.0	0.5 ± <0.1	102.0	0.5 ± <0.1	97.3	5.3
	1	1.0 ± <0.1	101.3	1.0 ± <0.1	95.3	1.1 ± <0.1	105.0	6.1
	5	4.9 ± <0.1	97.9	5.1 ± <0.1	101.6	4.8 ± 0.1	96.9	2.5
lake water	0							
	0.5	0.5 ± <0.1	101.3	0.48 ± <0.1	99.3	0.5 ± <0.1	104.7	5.2
	1	1.0 ± 0.1	99.3	1.0 ± 0.1	95.3	0.8 ± 0.1	84.3	9.2
	5	4.6 ± 0.2	92.3	4.9 ± 0.1	97.0	5.1 ± 0.1	102.3	5.1
apple	0							
	5	4.7 ± 0.3	93.2	4.8 ± 0.5	96.4	4.8 ± 0.3	95.8	6.9
	10	10.2 ± 1.0	102.1	9.7 ± 0.8	96.7	10.6 ± 0.8	105.6	8.3
	20	19.5 ± 0.4	97.7	18.6 ± 0.2	92.8	19.6 ± 1.9	97.9	5.7
pear	0							
	5	5.1 ± 0.3	102.9	4.8 ± 0.1	96.1	5.2 ± 0.3	103.5	5.6
	10	10.6 ± 0.4	105.9	10.2 ± 0.7	101.8	10.0 ± 0.3	99.5	5.0
	20	19.6 ± 1.0	97.8	21.1 ± 1.7	105.7	21.1 ± 0.1	105.6	6.1
tea powder	0							
	5	5.0 ± 0.5	100.3	5.1 ± 0.2	101.2	5.1 ± 0.5	102.5	7.7
	10	10.1 ± 0.3	100.5	10.6 ± 0.4	105.9	9.0 ± 0.5	90.2	7.9
	20	21.3 ± 0.2	106.7	19.0 ± 2.8	94.9	19.0 ± 1.0	95.05	9.5

[a]SD, standard deviation; RSD, relative standard deviation. Schematic description of the AChE modulated UCNPs-Cu^{2+} biosensor for organophosphorus pesticides detection.

DOI: 10.1021/acs.jafc.8b07201
J. Agric. Food Chem. 2019, 67, 4071−4079

laser excitation, Yb^{3+} was excited to the $^2F_{5/2}$ state. Because of the presence of Cu^{2+} in the close vicinity of upconverting nanocrystals and the $^1D_2$ level of the Cu^{2+} ions being close to the $^2F_{5/2}$ level, Cu^{2+} ions were excited by the sensitization of Yb^{3+}-trimmers and then relaxed to the ground state through a nonradiative way. Therefore, the energy transfer efficiency between Yb^{3+} and Tm^{3+} ions has been reduced as well as leading to reduction in the fluorescence emission intensity. To confirm further, the corresponding quenching performances of different concentration of copper ions toward PEI-capped UCNPs were also studied. The FL quenching effect of PEI-capped UCNPs were gradually increased with the incremental concentration of Cu^{2+} and when the concentration reached over 5 μM, the increasing of quenching efficiency was not significant indicating that chelating sites were almost saturated with the Cu^{2+}, as shown in Figure 3D. Therefore, 5 μM Cu^{2+} was selected as the optimum concentration for this experiment. In addition, we also investigated the effects of other cations (Ba^{2+}, Ca^{2+}, Mg^{2+}, Zn^{2+}, Na^+, K^+, NH_4^+, Cd^{2+}, Hg^{2+}, Mn^{2+}, Ag^+) on the fluorescent signal of PEI-capped UCNPs. As shown in Figure S2B, in the presence of other cations, tiny FL intensity changes were observed compared with Cu^{2+}, suggested the physiologically important other cations have negligible interference on the FL quenching of Yb^{3+}. All of these results observed above have ruled out the feasibility of other quenching process and recommended the ET mechanism.

3.3. Parameter Optimization. To achieve optimum detection performances for OPs, several related parameters including the incubation time of PEI-capped UCNPs and Cu^{2+}, the concentration of AChE, the reaction time of AChE and ATCh, temperature, and pH value of the system, and the reaction time upon addition pesticides were optimized in this experiment. The FL changes of 0.18 mg/mL PEI-capped UCNPs and 5 μM Cu^{2+} mixture under different incubation time were shown in Figure 4A. The FL emission intensity of UCNPs gradually decreases as the incubation time increases, and it became stable when reached to 6 min. Therefore, 6 min incubation time was selected for the subsequent experiments. Moreover, the effect of AChE enzyme concentration on the fluorescence signal of UCNPs sensor has also been investigated. Figure 4C showed the FL intensity of the UCNPs was gradually increased with the increasing concentration of AChE. Figure 4D revealed the variety of the fluorescence enhancement at different concentration of AChE. The FL enhancement was calculated using the equation: $E = (F-F_0)/F_0$, where F and F_0 represented the FL intensities at 800 nm in the presence and absence of AChE. A good linear relationship between fluorescence enhancement and AChE concentration was obtained in the range from 0.1 to 25 mU/mL. The regression equation was $(F-F_0)/F_0 = 0.0627[AChE] + 0.2629$ with the correlation coefficient (R^2) of 0.98. To obtain high sensitivity, 25 mU/mL was selected as the final concentration of AChE for the pesticides detection. We also investigated the effect of incubation time of UCNPs-Cu^{2+}-AChE in the presence of ATCh. As shown in Figure 4B, the FL intensity was gradually increased over time and achieved stable when the reaction time reached 30 min. Therefore, 30 min was selected as the optimum reaction time. Considering the activity of AChE enzyme is influenced greatly by temperature and pH, to promote the detection sensitivity of the proposed sensing strategy, we also further studied the effect of temperature and pH. The experiment results were presented in Figure S3A,B. The FL emission intensity of UCNPs-Cu^{2+}-AChE-ATCh system reached a maximum when the pH and the temperature reached at 8.0 and 37 °C, respectively. Therefore, pH 8.0 and temperature 37 °C were chosen for the following experiment. Finally, Figure S4 showed the changing trend of FL intensity with the reaction time upon addition of pesticides and the FL intensity was decreased gradually and remained fairly steady when the reaction time reached to 25 min. Therefore, 25 min reaction time was considered for the further experiments.

3.4. Sensitive Assay for OPs. The sensitivity of the developed sensor is one of the significant factors in detection. To ascertain the performance of this constructed biosensor, which was applied to determine the concentration of OPs under the optimum experimental conditions. When diazinon as a representative of OPs was added to the UCNPs-Cu^{2+}-ATCh-AChE system, it promoted the quench of FL intensity owing to the retardation of enzymatic reaction by diazinon. Figure 5A showed the upconversion FL spectra changes of the UCNPs in the presence of various concentrations of diazinon. As could be seen from the figure, the FL intensity at 800 nm decreased gradually with the increasing concentrations of the target molecules (diazinon). The plot of inhibition efficiency (*IE*, $IE = (F_0 - F)/F_0$, F_0 and F denote the FL intensity at 800 nm in the absence and presence of diazinon, respectively) against the concentrations of diazinon was shown in Figure 5B. A good linear relationship between the inhibition efficiency and the concentration (logarithm) of the diazinon was achieved over the ranges from 0.1 to 50 ng/mL. The calibration curve can be expressed as the equation, *IE* (inhibition efficiency, %) = 18.217(x = logarithm of the diazinon concentration) + 18.487 with R^2 0.985. The calculated limit of detection (LOD) of the biosensor for diazinon was 0.05 ng/mL (S/N = 3), which was extremely lower than the maximum residue limit of diazinon in food as reported in the Chinese National food safety standards (GBT 2763−2016) and the U.S. Department of Agriculture (0.01 ppm). Therefore, the constructed biosensor could be applied for the determination of diazinon in food samples to fulfill the requirements. In addition, a comparison between the developed biosensor and other reported methods for the determination of OPs was presented in Table S1, indicated that the proposed AChE modulated UCNPs-Cu^{2+} biosensor exhibited superior sensitivity to OPs compared with other reported methods.

3.5. Selectivity and Anti-interference Ability. It is pivotal to estimate the selectivity and anti-interference ability of the established biosensor for evaluating the determination performance of a method. First, diazinon (10 ng/mL) and some other common existing substances, including NaCl, $MgCl_2$, Na_3PO_4, $AlCl_3$, $CaCl_2$, glucose, cysteine, arginine, and vitamin C in food samples (10 μg/mL in the system), were mixed together to assess the anti-interference ability. As shown in Figure 6, the AChE modulated UCNPs-Cu^{2+} biosensor still had the same response to diazinon in the presence of interfering substances, which clearly indicated that there was negligible influence on diazinon detection. Meanwhile, it can also be observed that there were no significant inhibition efficiency changes when 10 μg/mL of above-mentioned common existing substances were added alone into system. In contrast, the biosensing system displayed an obvious FL intensity decrease upon addition of 10 ng/mL diazinon, indicating that the developed sensing strategy could provide good selectivity for the detection of diazinon. Second, to further investigate the specificity of the UCNPs biosensor for

DOI: 10.1021/acs.jafc.8b07201
J. Agric. Food Chem. 2019, 67, 4071−4079

the detection of OPs, some other commonly used pesticides such as fipronil, fenvalerate, cyfluthrin, bifenthrin, 2, 4-D, pymetrozine, and thiram were chosen as the interfering pesticides. As illustrated in Figure S5, only diazinon caused obvious inhibition efficiencies of the biosensing system and the other typical pesticides mentioned above at the same concentration of 10 ng/mL resulted in negligible interferences. Thus, all these results above vividly indicated that the prepared fluorescence sensing platform possessed high specificity and excellent anti-interference ability for OPs detection.

3.6. Evaluation of Accuracy. To evaluate the accuracy of the proposed AChE modulated UCNPs-Cu^{2+} biosensor for the determination of diazinon levels in real samples, a series of the spiked known amounts of diazinon in tap water, lake water, pretreated apple, pear, and tea powder were detected and investigated. All five matrices at four spiked concentrations were analyzed successively for 3 days. Meanwhile, interday relative standard deviation (RSD) were calculated to evaluate the reproducibility of the sensor. As shown in Table 1, excellent recoveries in the range from 84.3% to 105.9% with an interday RSDs (n = 9) of 2.5% to 9.5% were obtained. These results confirmed that the established method possess good precision and has high potential to detect diazinon in environmental samples and agricultural products as well.

3.7. Analytical Application in Authentic Samples. To further verify the practicability of the proposed FL method, seven apple samples sprayed randomly with different amount of diazinon were analyzed by GC−MS and this method simultaneously. The difference between achieved results of proposed FL biosensor and GC−MS method were not significant (p > 0.05), as shown in Table S2. These results suggested that the assay in this paper has the great potential applicability for OPs residues detection in real samples. In summary, a novel AChE modulated UCNPs-Cu^{2+} biosensor for the determination of organophosphorus pesticides in agricultural and environmental samples was successfully constructed in this study. There was no need for cumbersome UCNPs surface modification processes, as well as the synthesis of specific FL quenchers, this sensing system has many advantages including simplicity, environment friendly, easy to operate, and high stability. It is expected that the convenient strategy developed from this work could serve as a promising platform for the on-site detection of OPs in the future.

■ ASSOCIATED CONTENT

Supporting Information

The Supporting Information is available free of charge on the ACS Publications website at DOI: 10.1021/acs.jafc.8b07201.

Chemical and photostability of prepared PEI-capped UCNPs; influences of several related factors on performance of this biosensor; fluorescent emission intensity of UCNPs-Cu^{2+}-AChE-ATCh system; effects of incubation time on fluorescence responses of UCNPs-Cu^{2+}-AChE-ATCh system to pesticides detection; selectivity of proposed biosensor toward OPs against other pesticides; comparison of analytical performances of developed method with that of reported methods for diazinon detection; comparison of results from GC−MS and developed method for diazinon detection in authentic apple samples (PDF)

■ AUTHOR INFORMATION

Corresponding Author

*E-mail: qschen@ujs.edu.cn. Phone: +86-511-88790318. Fax: +86-511-88780201.

ORCID

Zheng-Zhu Zhang: 0000-0003-1564-1428

Quansheng Chen: 0000-0003-2498-3278

Funding

This study was financially supported by the National Natural Science Foundation of China (31772063), Key R&D Project of Jiangsu Province (BE2017357, BE2018307), and the Open Fund of State Key Laboratory of Tea Plant Biology and Utilization (SKLTOF20170113).

Notes

The authors declare no competing financial interest.

■ ACKNOWLEDGMENTS

The authors are thankful to the authorities of Jiangsu University for providing research facilities to carry out this work.

■ REFERENCES

(1) Valente, N. I. P.; Tarelho, S.; Castro, A. L.; Silvestre, A.; Teixeira, H. M. Analysis of organophosphorus pesticides in whole blood by GC-MS-μECD with forensic purposes. *J. Forensic Leg. Med.* **2015**, *33*, 28−34.

(2) Long, Q.; Li, H.; Zhang, Y.; Yao, S. Upconversion nanoparticle-based fluorescence resonance energy transfer assay for organophosphorus pesticides. *Biosens. Bioelectron.* **2015**, *68*, 168−174.

(3) Nanda Kumar, D.; Alex, S. A.; Chandrasekaran, N.; Mukherjee, A. Acetylcholinesterase (AChE)-mediated immobilization of silver nanoparticles for the detection of organophosphorus pesticides. *RSC Adv.* **2016**, *6*, 64769−64777.

(4) Hou, J.; Tian, Z.; Xie, H.; Tian, Q.; Ai, S. A fluorescence resonance energy transfer sensor based on quaternized carbon dots and Ellman's test for ultrasensitive detection of dichlorvos. *Sens. Actuators, B* **2016**, *232*, 477−483.

(5) Wang, Y.; Zhang, S.; Du, D.; Shao, Y.; Li, Z.; Wang, J.; Engelhard, M. H.; Li, J.; Lin, Y. Self assembly of acetylcholinesterase on a gold nanoparticles−graphene nanosheet hybrid for organophosphate pesticide detection using polyelectrolyte as a linker. *J. Mater. Chem.* **2011**, *21*, 5319−5325.

(6) Luo, Q.; Lai, J.; Qiu, P.; Wang, X. An ultrasensitive fluorescent sensor for organophosphorus pesticides detection based on RB-Ag/Au bimetallic nanoparticles. *Sens. Actuators, B* **2018**, *263*, 517−523.

(7) Huo, D.; Li, Q.; Zhang, Y.; Hou, C.; Lei, Y. A highly efficient organophosphorus pesticides sensor based on CuO nanowires−SWCNTs hybrid nanocomposite. *Sens. Actuators, B* **2014**, *199*, 410−417.

(8) Yan, X.; Song, Y.; Zhu, C.; Li, H.; Du, D.; Su, X.; Lin, Y. MnO_2 Nanosheet-Carbon Dots Sensing Platform for Sensitive Detection of Organophosphorus Pesticides. *Anal. Chem.* **2018**, *90*, 2618−2624.

(9) Yi, Y.; Gangbing, Z.; Chang, L.; Yan, H.; Youyu, Z.; Haitao, L.; Jiangna, Z.; Shouzhuo, Y. A label-free silicon quantum dots-based photoluminescence sensor for ultrasensitive detection of pesticides. *Anal. Chem.* **2013**, *85*, 11464−11470.

(10) Yu, T.; Ying, T. Y.; Song, Y. Y.; Li, Y. J.; Wu, F. H.; Dong, X. Q.; Shen, J. S. A highly sensitive sensing system based on photoluminescent quantum dots for highly toxic organophosphorus compounds. *RSC Adv.* **2014**, *4*, 8321−8327.

(11) Zhang, N.; Yanmei, S.; Zongzhao, S.; Shuai, L.; Shuying, L.; Yuehe, L.; Hua, W. Lab-on-a-drop: biocompatible fluorescent nanoprobes of gold nanoclusters for label-free evaluation of phosphorylation-induced inhibition of acetylcholinesterase activity

towards the ultrasensitive detection of pesticide residues. *Analyst* **2014**, *139*, 4620−4628.
(12) Harshit, D.; Charmy, K.; Nrupesh, P. Organophosphorus pesticides determination by novel HPLC and spectrophotometric method. *Food Chem.* **2017**, *230*, 448−453.
(13) Skowron, M.; Zakrzewski, R.; Ciesielski, W. Application of image analysis technique for the determination of thiophanate methyl by thin-layer chromatography. *J. Planar Chromatogr.–Mod. TLC* **2016**, *29*, 221−226.
(14) Piao, Y. Z.; Kim, Y. J.; Kim, Y. A.; et al. Development of ELISAs for the Class-Specific Determination of Organophosphorus Pesticides. *J. Agric. Food Chem.* **2009**, *57*, 10004−10013.
(15) Xie, J.; Liu, T.; Song, G.; Hu, Y.; Deng, C. Simultaneous Analysis of Organophosphorus Pesticides in Water by Magnetic Solid-Phase Extraction Coupled with GC−MS. *Chromatographia* **2013**, *76*, 535−540.
(16) Sgobbi, L. F.; Machado, S. A. S. Functionalized polyacrylamide as an acetylcholinesterase-inspired biomimetic device for electrochemical sensing of organophosphorus pesticides. *Biosens. Bioelectron.* **2018**, *100*, 290−297.
(17) Bala, R.; Sharma, R. K.; Wangoo, N. Development of gold nanoparticles-based aptasensor for the colorimetric detection of organophosphorus pesticide phorate. *Anal. Bioanal. Chem.* **2016**, *408*, 1−6.
(18) Tan, M. J.; Hong, Z. Y.; Chang, M. H.; Liu, C. C.; Cheng, H. F.; Xian, J. L.; Chen, C. H.; Liao, C. D.; Kong, K. V. Metal carbonyl-gold nanoparticle conjugates for highly sensitive SERS detection of organophosphorus pesticides. *Biosens. Bioelectron.* **2017**, *96*, 167−172.
(19) Wei, J.; Cao, J.; Hu, H.; Yang, Q.; Yang, F.; Wan, J.; Su, H.; He, C.; Li, P.; Wang, Y. Sensitive and Selective Detection of Oxo-Form Organophosphorus Pesticides Based on CdSe/ZnS Quantum Dots. *Molecules* **2017**, *22*, 1421.
(20) Pan, W.; Zhao, J.; Chen, Q. Fabricating Upconversion Fluorescent Probes for Rapidly Sensing Foodborne Pathogens. *J. Agric. Food Chem.* **2015**, *63*, 8068−8074.
(21) Liu, Y.; Ouyang, Q.; Li, H.; Chen, M.; Zhang, Z.; Chen, Q. Turn-On Fluoresence Sensor for Hg^{2+} in Food Based on FRET between Aptamers-Functionalized Upconversion Nanoparticles and Gold Nanoparticles. *J. Agric. Food Chem.* **2018**, *66*, 6188−6195.
(22) Li, H.; Chen, Q.; Zhao, J.; Urmila, K. Fabricating upconversion fluorescent nanoparticles modified substrate for dynamical control of cancer cells and pathogenic bacteria. *J. Biophotonics.* **2017**, *10*, 1034−1042.
(23) Li, J.; Hong, X.; Li, D.; Zhao, K.; Wang, L.; Wang, H.; Du, Z.; Li, J.; Bai, Y.; Li, T. Mixed ligand system of cysteine and thioglycolic acid assisting in the synthesis of highly luminescent water-soluble CdTe nanorods. *Chem. Commun.* **2004**, *15*, 1740−1741.
(24) Liu, D.; Chen, W.; Wei, J.; Li, X.; Wang, Z.; Jiang, X. A highly sensitive, dual-readout assay based on gold nanoparticles for organophosphorus and carbamate pesticides. *Anal. Chem.* **2012**, *84*, 4185−4191.
(25) Kumar, D. N.; Alex, S. A.; Kumar, R. S. S.; Chandrasekaran, N.; Mukherjee, A. Acetylcholinesterase inhibition-based ultrasensitive fluorometric detection of malathion using unmodified silver nanoparticles. *Colloids Surf., A* **2015**, *485*, 111−117.
(26) Kim, M.; Lee, K.; Kwon, J. E.; Koh, W. G. Signal-amplifying nanoparticle/hydrogel hybrid microarray biosensor for metal-enhanced fluorescence detection of organophosphorus compounds. *Biofabrication* **2018**, *10*, 1758−5090.
(27) Hou, J.; Dong, J.; Zhu, H.; Xue, T.; Ai, S.; Mang, M. A simple and sensitive fluorescent sensor for methyl parathion based on l -tyrosine methyl ester functionalized carbon dots. *Biosens. Bioelectron.* **2015**, *68*, 20−26.
(28) Lin, B.; Yan, Y.; Guo, M.; Cao, Y.; Yu, Y.; Zhang, T.; Huang, Y.; Wu, D. Modification-free carbon dots as turn-on fluorescence probe for detection of organophosphorus pesticides. *Food Chem.* **2018**, *245*, 1176−1182.
(29) Wu, X.; Song, Y.; Yan, X.; Zhu, C.; Ma, Y.; Du, D.; Lin, Y. Carbon quantum dots as fluorescence resonance energy transfer sensors for organophosphate pesticides determination. *Biosens. Bioelectron.* **2017**, *94*, 292−297.
(30) Song, Y.; Yan, X.; Li, Z.; Qu, L.; Zhu, C.; Ye, R.; Li, S.; Du, D.; Lin, Y. Highly photoluminescent carbon dots derived from linseed and their applications in cellular imaging and sensing. *J. Mater. Chem. B* **2018**, *6*, 3181−3187.
(31) Fang, A.; Qian, L.; Wu, Q.; Li, H.; Zhang, Y.; Yao, S. Upconversion nanosensor for sensitive fluorescence detection of Sudan I−IV based on inner filter effect. *Talanta* **2016**, *148*, 129−134.
(32) Ouyang, Q.; Liu, Y.; Chen, Q.; Guo, Z.; Zhao, J.; Li, H.; Hu, W. Rapid and specific sensing of tetracycline in food using a novel upconversion aptasensor. *Food Control* **2017**, *81*, 156−163.
(33) Guo, T.; Deng, Q.; Fang, G.; Gu, D.; Yang, Y.; Wang, S. Upconversion fluorescence metal-organic frameworks thermo-sensitive imprinted polymer for enrichment and sensing protein. *Biosens. Bioelectron.* **2016**, *79*, 341−346.
(34) Sedlmeier, A.; Hlavã, Ä. e. A.; Birner, L.; Mickert, M. J.; Muhr, V.; Hirsch, T.; Corstjens, P. L.; Tanke, H. J.; Soukka, T.; Gorris, H. H. Highly Sensitive Laser Scanning of Photon-Upconverting Nanoparticles on a Macroscopic Scale. *Anal. Chem.* **2016**, *88*, 1835−1841.
(35) Hu, W.; Chen, Q.; Li, H.; Qin, O.; Zhao, J. Fabricating a novel label-free aptasensor for acetamiprid by fluorescence resonance energy transfer between NH_2 -$NaYF_4$: Yb, ho@SiO_2 and Au nanoparticles. *Biosens. Bioelectron.* **2016**, *85*, 997−997.
(36) You, H.; Hua, X.; Feng, L.; Sun, N.; Qi, R.; Wang, L.; Wang, M. Competitive immunoassay for imidaclothiz using upconversion nanoparticles and gold nanoparticles as labels. *Microchim. Acta* **2017**, *184*, 1−8.
(37) Si, F.; Zou, R.; Jiao, S.; Qiao, X.; Guo, Y.; Zhu, G. Inner filter effect-based homogeneous immunoassay for rapid detection of imidacloprid residue in environmental and food samples. *Ecotoxicol. Environ. Saf.* **2018**, *148*, 862−868.
(38) Wang, F.; Chatterjee, D. K.; Li, Z.; Zhang, Y.; Fan, X.; Wang, M. Synthesis of polyethylenimine/$NaYF_4$ nanoparticles with upconversion fluorescence. *Nanotechnology* **2006**, *17*, 5786−5791.
(39) Chen, G.; Ohulchanskyy, T. Y.; Rajiv, K.; Hans, A.; Prasad, P. N. Ultrasmall monodisperse $NaYF_4Yb^{3+}/Tm^{3+}$ nanocrystals with enhanced near-infrared to near-infrared upconversion photoluminescence. *ACS Nano* **2010**, *4*, 3163−3168.
(40) Sun, J.; Yang, X. Gold nanoclusters−Cu^{2+} ensemble-based fluorescence turn-on and real-time assay for acetylcholinesterase activity and inhibitor screening. *Biosens. Bioelectron.* **2015**, *74*, 177−182.
(41) Gao, Z. F.; Li, T. T.; Xiao, L. X.; Yi, Y. L.; Hong, Q. L.; Li, N. B. Green light-emitting polyepinephrine-based fluorescent organic dots and its application in intracellular metal ions sensing. *Biosens. Bioelectron.* **2016**, *83*, 134−141.
(42) Wang, F.; Zhang, C.; Qin, X.; Li, H.; Xian, Y. Label-free Upconversion Nanoparticles-based Fluorescent Probes for Sequential Sensing of Cu^{2+}Pyrophosphate and Alkaline Phosphatase Activity. *Biosens. Bioelectron.* **2017**, *95*, 21−26.
(43) Sarkar, S.; Manjunath, C.; Venkataramanan, M. Highly luminescent colloidal Eu^{3+}-doped $KZnF_3$ nanoparticles for the selective and sensitive detection of Cu^{II} ions. *Chem. - Eur. J.* **2014**, *20*, 3311−3316.

DOI: 10.1021/acs.jafc.8b07201
J. Agric. Food Chem. 2019, 67, 4071−4079